Int. J. Electrochem. Sci., 5 (**2010**) 407 - 413

International Journal of ELECTROCHEMICAL SCIENCE
www.electrochemsci.org

Contrasting Underpotential Depositions of Lead and Cadmium on Silver Macroelectrodes and Silver Nanoparticle Electrode Arrays

Fallyn W. Campbell and Richard G. Compton[*]

Department of Chemistry, Physical and Theoretical Chemistry Laboratory, University of Oxford,
South Parks Road, Oxford OX1 3QZ, United Kingdom
[*]E-mail: richard.compton@chem.ox.ac.uk

Received: 12 Marc 2010 / *Accepted:* 20 March 2010 / *Published:* 31 March 2010

In this paper we report behaviour of contrasting underpotential deposition of lead and cadmium on silver. UPD is observed at the macroscale and for silver nanoparticles (AgNPs) with diameter greater than *ca.* 50 nm, however, the same behaviour is absent for NPs with diameter below *ca.* 50nm.

Keywords: Silver nanoparticles, underpotential deposition, lead, cadmium

1. INTRODUCTION

The study of nanomaterials is continually expanding area of research with nanoparticles finding a variety of applications in sensing and catalysis [1,2]. Nanoparticles are known to possess a variety of features differing from their corresponding bulk material including enhanced mass transport due to convergent diffusion, improved signal – to – noise ratio and increased active surface area. However, the adsorption of species on nanoparticulate material is still relatively unexplored by comparison. This is an important area to consider as the reduction in size can lead to changed electronic and surface properties, with crystal faces exposed that would not be seen at the macroscale. Previous studies carried out in our laboratory have demonstrated a size – dependent adsorption of thallium metal on colloidal silver nanoparticles [3] and gold nanoparticles supported on carbon nanotubes [4].

Study of the deposition of metals can be important in the understanding of adsorbate – substrate interaction, in the design of bi – metallic catalysts and the study of alloys. A variety of metals have been reported to adsorb on silver substrates including thallium [5], bismuth, copper [6], lead [7], nickel [8], zinc [9] and cadmium [10]. The simultaneous deposition of lead and thallium on polycrystalline silver electrodes [11] appears to be strongly dependent on the composition of supporting electrolyte.

The presence of adsorbing anions in solution can also affect the deposition process [12,13]. Furthermore, UPD of lead and cadmium adsorbates has been examined on gold and silver single crystal surfaces [11, 14, 15, 16] as well as modified silver electrodes [17]. Results of such studies have indicated deposition can be very sensitive to the solution composition and the electrode surface structure. Similarly, the work functions associated with the substrate material and the deposit may also be related to the particle size.

Examples of nanoparticles size - effects in electrochemical studies includes altered kinetics for the electrocatalytic reduction of oxygen [18], the size – dependent charging of gold nanoparticles [19], improved tolerance to electrode fouling [20] and varied capacity for hydrogen storage [21, 22], depending on particle size.

In this paper we focus on the electrochemical underpotential and bulk deposition of lead and cadmium on silver macroelectrodes and AgNP arrays composed of varying sizes of particles. The reduction of lead and cadmium to an adsorbed layer of metal is represented by Equations (1) and (2), respectively. In particular we examine the UPD process which can be distinguished from that of the bulk deposition, in both cases, at potentials positive of the reversible Nernst potential.

$$Pb^{2+} + 2e^{-} \rightleftharpoons Pb_{(metal)} \tag{1}$$

$$Cd^{2+} + 2e^{-} \rightleftharpoons Cd_{(metal)} \tag{2}$$

Specifically we are concerned with size – dependent adsorption behaviour exhibited by silver nanoparticles in the UPD region. This in turn leads to altered UPD behaviour between the macro and nanoscale.

2. RESULTS AND DISCUSSION

Cyclic voltammetry for the deposition of lead at a silver macrodisk is shown in Figure 1. A distinct UPD process is recognizable at E_p = - 0.43 V, with formation of a sub-monolayer, and the corresponding stripping peak at – 0.39 V. The bulk deposition of lead takes place on silver electrode at potentials negative of – 0.6 V, with the corresponding stripping peak at – 0.54 V. The bulk deposition does not produce a distinct peak but rather appears as a continuation of the UPD peak. The number of layers deposited in bulk process can be increased by extending the deposition time or by scanning to a more negative potential. We are able to record only the UPD peak without any bulk deposition by scanning from 0 to – 0.6 V and reversing the scan direction.

The lead deposition at a silver nanoparticle array is shown in Figure 2. The solid line shows the voltammetry obtained for large AgNPs (80 – 120nm) and the dashed line shows the same for smaller particles (20 - 40 nm). It is clear that for the larger nanoparticles as for the macrodisk, distinct underpotential deposition and stripping peaks are observed at – 0.43 V and – 0.39 V respectively. On the other hand, for the small AgNPs distinctive deposition and stripping peaks are absent in UPD region.

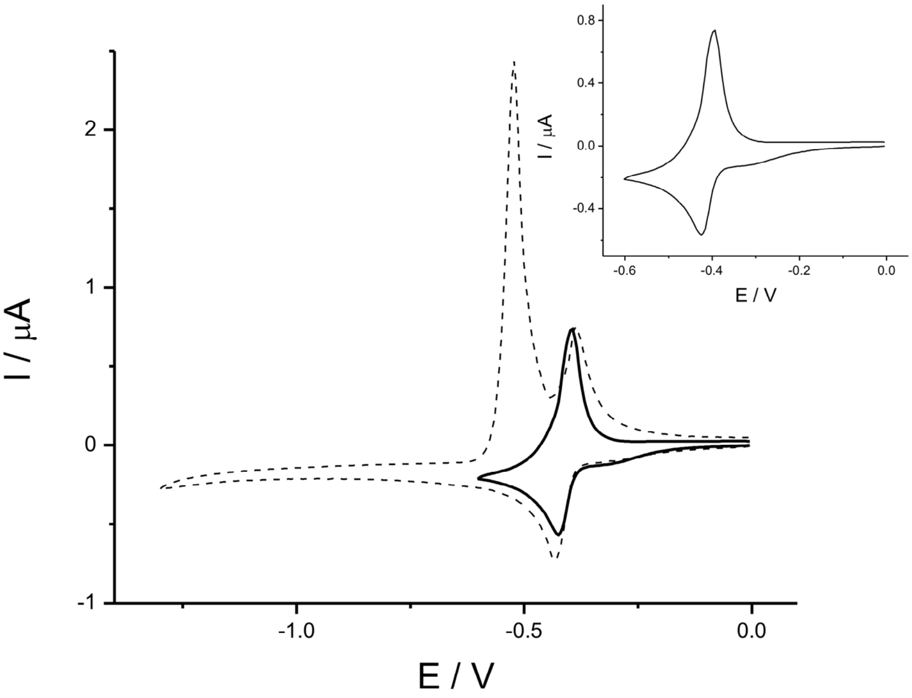

Figure 1. Lead deposition on silver macrodisk electrode (area = 3.85 x 10 $^{-3}$ cm^2) from a solution of sodium potassium tartrate (0.1 M) + H_2SO_4 (0.01M) + $Pb(NO_3)_2$ (3 x 10 $^{-3}$ M). Scan rate: 50 mVs^{-1}, vs. SCE. (Inset: magnification of the solid line showing only UPD region).

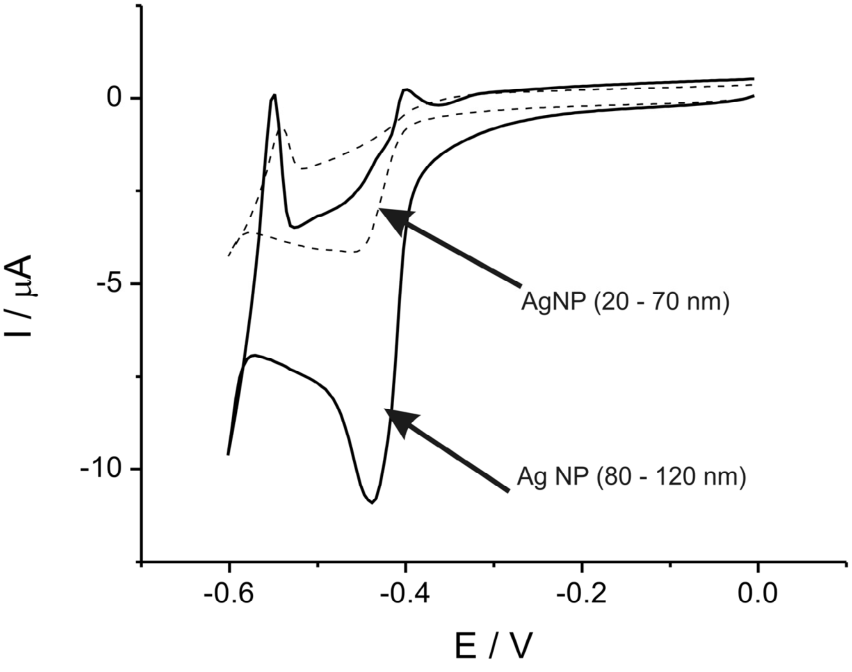

Figure 2. Lead deposition on silver nanoparticle modified BPPG electrode. Solid line: AgNP – BPPG 80 -120 nm; Dashed line: AgNP – BPPG 20 – 70 nm. Scan rate: 50 mVs^{-1}, vs. SCE.

A similar behaviour can be observed for the deposition of cadmium on silver electrodes. The deposition of cadmium on a silver macroelectrode is displayed in Figure 3. The bulk deposition takes place at – 0.77 V with corresponding stripping peak at – 0.72 V. The UPD process takes place – 0.57 V, with stripping at – 0.55 V. We are able to record the isolated UPD process by scanning negatively to – 0.7 V and reversing the scan direction.

We then considered AgNP arrays composed of 80 -120 nm diameter nanoparticles. In this case we once again observed UPD behaviour, similar to that occurring at the silver macroelectrode. Figure 4 displays the behaviour of AgNP – BPPG (80 – 120 nm) as a solid line with underpotential deposition taking place at potentials very close to that of the macroelectrode, with deposition taking place at – 0.56 V and stripping at – 0.54 V. The dashed line in Figure 4 shows the absence of distinctive cadmium UPD and stripping process for a AgNP – BPPG (20 – 40 nm). The sharp peaks superimposed on the deposition/stripping waves may be due to deposition on different crystal faces of the larger NPs.

In the case of both, lead and cadmium deposition on AgNPs, the intermediate nanoparticle size, 50 – 70 nm, behaves much like the smaller size (20 – 40 nm), with no obvious underpotential deposition process taking place.

The behaviour exhibited by silver nanoparticles of varying size toward the underpotential deposition of lead and cadmium is similar to that reported in our study of thallium UPD on silver nanoparticles [2].

In the case of the larger AgNPs (80 – 120 nm) it seems that more material is deposited than is stripped off in the underpotential region. This could possibly indicate the occurrence of alloy formation or an incomplete stripping process at the nano-scale material. This process may also contribute to the behaviour of the smaller NPs (20 – 40 nm). Resulting in the absence of distinct UPD / stripping features in the voltammerty. High surface energy of smaller NPs may promote alloying, incorporating deposited material into the particle making it inaccessible during the stripping step. This is a distinctly different behaviour from that observed at the macro-scale electrode.

3. CONCLUSIONS

Investigation of the electrochemical deposition of the heavy metals lead and cadmium on silver nanoparticles has allowed us to conclude that a minimum diameter of *ca.* 50 nm is required in order to clearly observe the underpotential deposition and corresponding stripping processes for both deposits. This process is absent for both lead and cadmium deposition where the array is composed of small silver nanoparticles, diameter less the *ca.* 50 nm. A similar situation has previously been reported for the underpotential deposition of thallium on large and small silver nanoparticles. We suggest this is a general behaviour for the case of underpotential deposition of heavy metals on silver nanomaterials; in particular the change of surface structure and / or work function at the nanoscale qualitatively alters the observed electrochemistry. We suggest there may also be a contribution from possible alloy formation or an incomplete stripping process taking place at the nano – scale. This process may contribute to the absence of distinct UPD / stripping peaks at the smaller NPs.

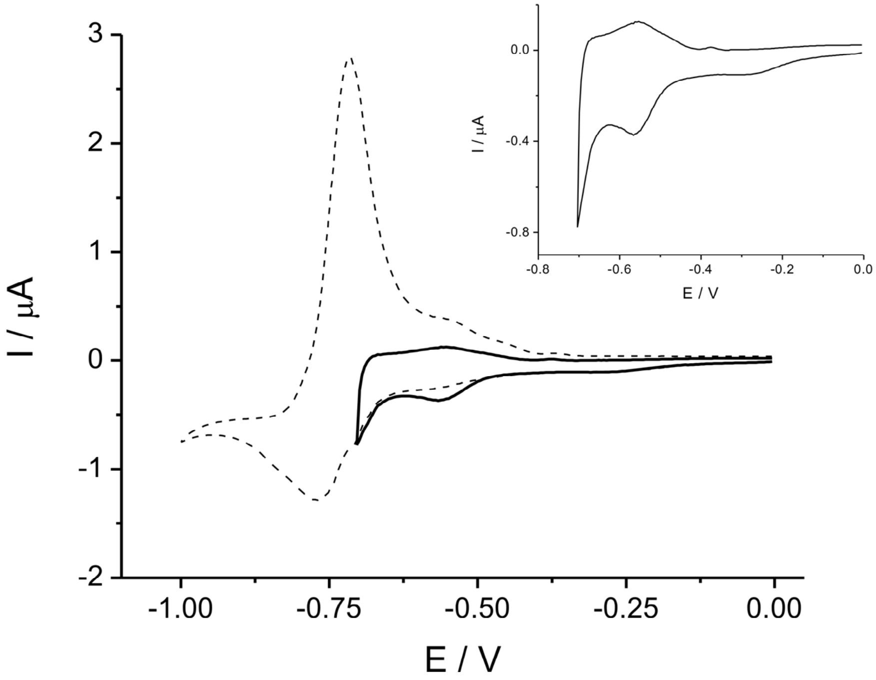

Figure 3. Cadmium deposition on a silver macrodisk electrode (area = 3.85 x 10 $^{-3}$ cm^2) from a solution of Na_2SO_4 (0.5 M) + H_2SO_4 (0.01 M) + $CdSO_4$ (2 x 10 $^{-3}$ M). Scan rate: 50 mVs^{-1}, vs. SCE. (Inset: magnification of solid line showing only UPD region).

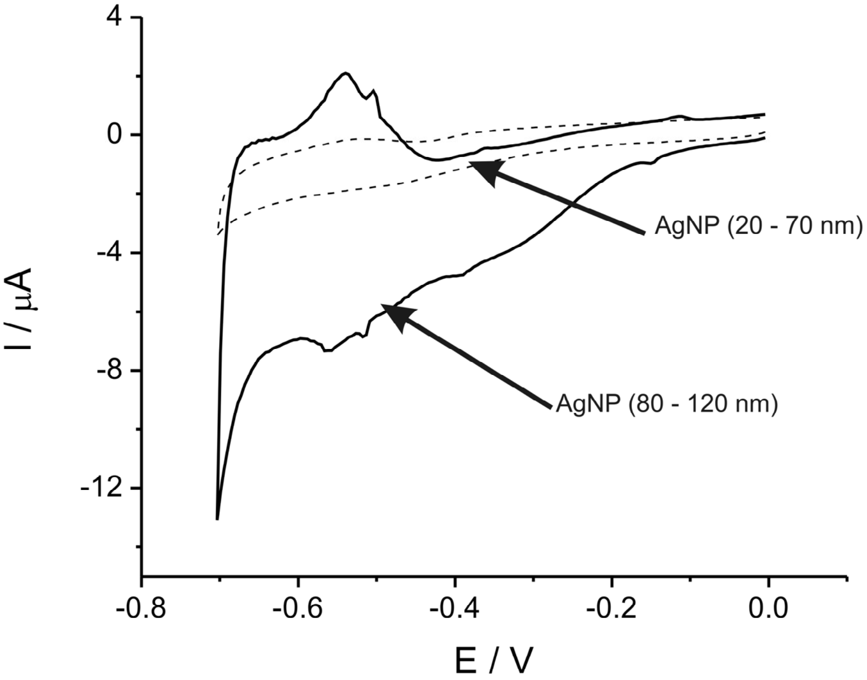

Figure 4. Cadmium deposition on silver nanoparticle modified BPPG electrode. Solid line: AgNP – BPPG 80 -120 nm; Dashed line: AgNP – BPPG 20 – 70 nm. Scan rate: 50 mVs^{-1}, vs. SCE.

4. EXPERIMENTAL PART

$Pb(NO_3)_2$ (99%, BDH), $CdSO_4$ (99%, Aldrich), $C_4H_4KNaO_6.4H_2O$ (99% , Fluka), H_2SO_4 (99%, Fisher Scientific), Na_2SO_4 (99% Aldrich) and $NaClO_4$ (98 – 102 %, Johnson Matthey) were used as received without further purification. All solutions were prepared using Millipore pure water with resistivity not less than 18.2 M Ω cm^{-1} at 25 °C (Vivendi Water Systems, UK).

All electrochemical experiments were performed using a μAutolab Type III potentiostat and desktop PC. A three - electrode set up was used consisting of working electrode, carbon rod counter electrode and saturated calomel (SCE) reference electrode (Radiometer Analytical). Carbon rods and basal plane pyrolytic graphite (BPPG) were supplied by Le Carbone, Sussex, UK. All electrolyte solutions were de-aerated with N_2 gas prior to experiments.

The AgNPs were synthesized by a seed mediated citrate reduction of $AgNO_3$ adapted from a procedure by Pyatenko [23, 24], and detailed in our previous publications [25, 26]. This method generated AgNPs with diameter 20 – 40 nm, 50 – 70 nm and 80 – 120 nm. Lead deposition was performed in $C_4H_4KNaO_6.4H_2O$ (0.1 M) + H_2SO_4 (0.01 M) + $Pb(NO_3)_2$ (0.3 mM) at 50 mVs^{-1} by scanning negatively from 0 to – 1.3 V and reversing the scan direction. Cadmium deposition was carried out in a solution of Na_2SO4 (0.5 M) + H_2SO_4 (0.01 M) + $CdSO_4$ (2 mM) at 50 mVs^{-1}, scanning negatively from 0 to – 1.0 V and reversing scan direction.

The as synthesized AgNP suspensions were then evaporated on the surface of a BPPG electrode, to fabricate the arrays. Following the deposition and stripping experiments the AgNPs were quantified by stripping from BPPG electrode by LSV in $NaClO_4$ (0.1 M), scanning from 0 V to 1.0 V at 20 mVs^{-1}.

ACKNOWLEDGMENTS
F. W. C. would like to thank EPSRC and Abington Partners, Bath for funding.

References

1. F. W. Campbell, R. G. Compton, *Anal. Bioanal. Chem.*, 396 (2010) 241.
2. C. M. Welch, R. G. Compton, *Anal. Bioanal. Chem.*, 384 (2006) 601.
3. F. W. Campbell, Y-G. Zhou, R. G. Compton, *New J. Chem.,* (2009) *in press* DOI: 10.1039/B9NJ00669A.
4. C. Batchelor – McAuley, G. G. Wildgoose and R. G. Compton, *New. J. Chem.*, 32 (2008) 941.
5. K.-O. Thiel, M. Hintze, A. Vollmer and C. Donner, *J. Electroanal. Chem.*, 621 (2008) 7.
6. S. P. E. Smith, H. D. Abruña, *J. Phys. Chem. B*, 103 (1999) 6764.
7. Y. V. Bokshits, N. P. Osipovich, E. A. Strel'tsov and G. P. Shevchenko, *Colloids and Surfaces A: Physicochem. Eng. Aspects,* 242 (2004) 79.
8. S. Morin, A. Lachenwitzer, F. A. Moller, O. M. Magnussen and R. J. Behm, *J. Electrochem. Soc.*, 146 (1999) 1013.
9. J. Miragliotta and T. E. Furtak, Surf. Interface Anal., 14 (1989) 53.
10. Y. Bonfil, M. Brand and E. Kirowa-Eisner, *Analytica Chimica Acta*, 464 (2002) 99.
11. S. Bharathi, V. Yegnaraman, G. Prabhakara Rao, *J. Appl. Electrochem.*, 24 (1994) 981.
12. V. D. Jović, B. M. Jović, A. R. Despić, *J. Electroanal. Chem.*, 288 (1990) 229.

13. V. D. Jović, B. M. Jović, *Electrochimica Acta*, 47 (2002) 1777.
14. M. F. Toney, J. G. Gordon, M. G. Samant, G. L. Borges, O. R. Melroy, *J. Phys. Chem.*, 99 (1995) 4733.
15. H. Bort, K. Jüttner, W. J. Lorenz, *Electrochimica Acta*, 28 (1983), 993.
16. L. P. Bicelli, B. Bozzini, C. Mele, L. D'Urzo, *Int. J. Electrochem. Sci.*, 3 (2008) 356.
17. J. W. F. Robertson, D. J. Tiani, J. E. Pemberton, *Langmuir*, 23 (2007) 4651.
18. H.Ye, J. A. Crooks, R. M. Crooks, *Langmuir*, 23 (2007) 11901.
19. A. Toyota, T. Sagara, *Electrochimica Acta*, 53 (2008) 2553.
20. F. Maillard, M. Martin, F. Gloaguen, J. –M. Léger, *Electrochimica Acta*, 47 (2002) 3431.
21. O. Friedrichs, L. Kolodziejczyk, J. C. Sánchez – López, A. Fernández, L. Lyubenova, D. Zander, U. Köster, K. F. Aguey – Zinsou, T. Klassen, R. Bormann, *J. Alloy. Compd.*, 463 (2008,) 539.
22. K. Zhong, Y. Liu, M. Gao, J. Wang, H. Miao, H. Pan, *Int. J. Hydrogen Energ.*, 33 (2008) 149.
23. A. Pyatenko, M, Yamaguchi, M. Suzuki, *J. Phys. Chem.*, 111 (2007) 7910.
24. A. Pyatenko, M, Yamaguchi, M. Suzuki, *J. Phys. Chem.*, 109 (2005) 21608.
25. F. W. Campbell, S. R. Belding, R. Baron, L. Xiao, R. G. Compton, *J. Phys. Chem. C*, 113 (2009) 14852.
26. F. W. Campbell, S. R. Belding, R. Baron, L. Xiao, R. G. Compton, *J. Phys. Chem. C*, 113 (2009) 9053.